IDENTIFYING SURFACE ANGLED CRACKS ON ALUMINIUM BAR USING EMATS AND AUTOMATED COMPUTER SYSTEM

M. H. Rosli[1], R. S. Edwards[1], B. Dutton[1], C. G. Johnson[2], and P. Cattani[2]

[1]Department of Physics, University of Warwick, Coventry, CV4 7AL, UK
[2]Computing Laboratory, University of Kent, Canterbury, CT2 7NF, UK

ABSTRACT. Electromagnetic acoustic transducers (EMATs) have been used in pitch-catch manner to identify surface cracking in aluminium bars and rails. The differences between signal enhancement due to interference produced by normal (90°) and angled cracks in B-scans were utilised to classify them in order to decide appropriate depth calibration curve for depth estimation. In addition, the B-scans were also used to determine the presence of any surface defects. The B-scans were input into image processing algorithm that select the best features and use it for training and recognising similar pattern in other B-scans.

Keywords: EMATs, Ultrasonic, Rayleigh waves
PACS: 81.70.Cv

INTRODUCTION

The presences of surface cracking in many metal structures raise the issue of their integrity. If not detected and treated at early stages, they are potentially causing disastrous consequences to human being and the environment [1-3]. For instance, gauge corner cracking (GCC), resulting from rolling contact fatigue (RCF) arise in rail tracks due to a combination of high normal and tangential stresses between wheel and the rail. GCC starts growing at shallow angle (20°-30°) to the surface to a few milimetres deep into the rail and potentially break it [1]. On the other hand, stress corrosion cracking (SCC), is a result of conjoint action of stress and corrosive environment [2]. It normally occurs in pipes, pressure vessels, steam-turbines and welding joints. Meanwhile, in manufacturing and steel casting industry the effect of chemical, process and engineering parameters contribute to the presence of surface defects which affects the quality of the product [4]. Clearly, the consequence of surface defects on these areas is catastrophic. Thus, a technique or process of detecting and identifying the surface cracking is paramount.

Standard ultrasonic method to inspect surface defects employs piezoelectric transducers to transmit and receive ultrasonic signal in pulse-echo mode. Piezoelectric transducers require a couplant such as gel or water to transfer the vibration to the test specimen. This becomes a problem when the environment has to be kept dry and clean during the inspection. Electromagnetic acoustic transducers (EMATs) works through different mechanism compared to piezoelectric. It is a contactless method which means EMATs can operate at a few milimetres stand-off from the sample and require no couplant to transfer the vibration [5, 6]. These can provide a clean contactless method that is potentially can be use for online high speed inspection. Besides that, the broadband nature of the signal generated by EMATs provides a wide range of depth it can probe into.

Current research shows interesting features in B-scans when scanning over surface angled cracks using EMATs in pitch-catch mode. Within close proximity of the crack, the

signals are enhanced but it is for much longer period than for normal cracks [7]. These features can be spotted through human observation, but it requires expertise and long working hours which is not reliable. Thus, image processing of the B-scans that executes automated classification of images helps to recognise the enhancement patterns and can be incorporated in the inspection system to increase its operation speed.

The main concept is, given a dataset consisting of images each of which has been tagged with one or more classes, to develop a classification program that will take a new image of that type and allocate it to one of the classes. Typically, this is done by a machine learning algorithm [8]. Machine learning algorithms take datasets and automatically construct a model in the form of, for example, a decision tree or list of rules, or a more complex model such as a computer program.

One of the more challenging aspects of this process is deciding which features of the image to extract to use as inputs to the classification algorithm. Raw pixel values are usually too numerous and too fine grained to offer a sensible set of inputs to the classifier. One approach is for an expert in the kind of images being studied to provide a set of features, and for bespoke programs to be written to extract those features. This is complex and time consuming, and dependent on the expert's knowledge. More recently, a number of authors have explored methods which apply machine learning methods to this feature extraction step, as well as to the classification itself [9-11]. These have typically been based on evolutionary algorithms, i.e. algorithms that take their inspiration from biological evolution.

ULTRASOUND TECHNIQUE

METHOD

EMAT generates ultrasonic waves in electrically conducting material via Lorentz mechanism and via magnetostrictive mechanism in magnetic material [6]. The principal method works in pitch-catch mode, where one EMAT with thick wire coil generates ultrasonic waves while another EMAT with thin wire coil receive the signal at a distance away. Since the main concern of this experiment is to detect surface cracks, the receive EMAT was specifically made to be more sensitive to surface waves. The combination of a pulse generator and the EMAT produce broadband ultrasonic waves ranging from 50-500kHz that has a centre frequency around 200kHz. At these frequencies, the surface waves generated are mainly Rayleigh waves since the thickness of the sample used are large enough. Rayleigh will be affected much by the surface cracks depending on the wavelength, hence it is vital to know its arrival time from the EMATs separation and its phase velocity in particular material. The phase velocity was referred from reference [12].

There are two ways of how the “pitch-catch” method was implemented. In preliminary experiments, a generation EMAT is fixed at 200mm from the surface crack opening corner while a receive EMAT is scanned with 0.5mm scan step away on the sample surface that contains cracks as shown in Figure 1(a). To get a strong signal, the generation EMAT was in contact with the sample while a layer of acetate with a line drawn on it was attached between the receive EMAT and the sample to mark the centre of the coil. In the second method, a trolley was used to hold both EMATs at 1mm stand-off from the sample surface and also fixing the separation between the EMATs. The pair of EMATs mounted on the trolley works as a unit and scanned on the sample surface. In order to characterise within close proximity of the surface defects, the unit is scanned with 0.5mm scan step.

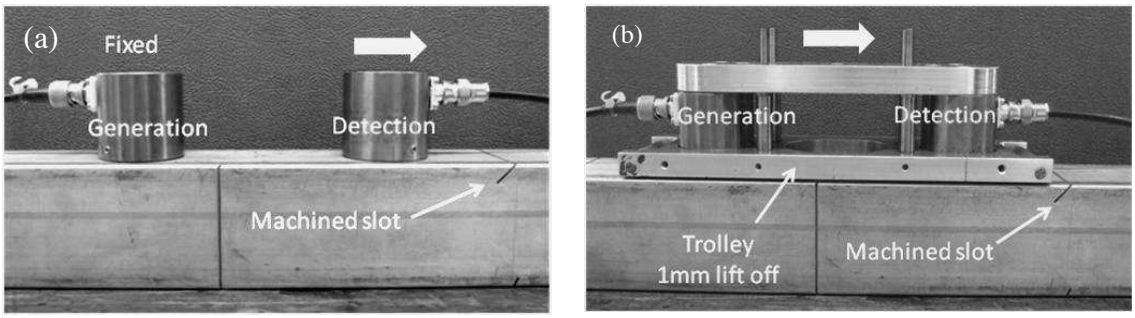

Figure 1 Pitch-catch mode of scanning the EMATs on aluminium bar containing machine slots (a) Scanning detection EMAT away from fixed generation EMAT (b) Fixing both EMATs on a trolley while scanning.

In order to simulate real life surface cracking such as GCC, a number of sample was made from aluminium bars with a few machined slots on the surface. Each slot has 1mm width and far enough from each other to allow for scanning using trolley and minimise the probability of reflections. The slots are inclined from the surface with angle, θ which range from normal, 90° to as shallow as 18° from the surface and the depth range from 0.5mm to 20mm.The actual lengths of the slots depend on θ and depth. In addition to aluminium bars, experiments have been done on a test rail track and on a section of rail track removed from service containing transverse cracks and GCC. The test rail track contains three clusters of electrical discharge machining (EDM) notches. Each cluster contains three notches at 25° of depth 2mm, 4mm and 10mm respectively. The only difference between the clusters is the separation between the notches which are 5mm, 10mm and 15mm each.

RESULTS

Normal and angled cracks

Surface cracks behave like a low-pass filter, where it blocks short wavelength Rayleigh wave and let longer wavelength wave pass through. When the EMATs are fixed on a trolley and scan over the sample surface, the amplitude of Rayleigh waves drop when it pass over a slot. The drop in amplitude was used for depth gauging by plotting normalised amplitude as a function of depth as shown in Figure 2. Normalised amplitude is defined as the amplitude at a particular point divide by the amplitude over a crack-free section. The depth calibration curve was plotted using the data recorded from scanning over six normal slots with various depths. As it shown, a negative exponential curve represents the data trend as the depth increases. This curve can be used to determine the depth of unknown cracks on the same material by interpolating their normalised amplitude.

However, when the data from angled slots are used to plot the depth calibration curve, the results shows that they are angle dependent. For example, Figure 2(b) shows the curve produced from 45° slots scans trace on the curve produced from normal slots scans. It shows that there is a discrepancy between the two curves. For given normalised amplitude, the 45° curve suggesting a much deeper slot compared to the normal slots curve. This could lead to a large error when estimating the depth of unknown crack. Thus, it is vital to know the orientation of the crack before using the right depth calibration curve.

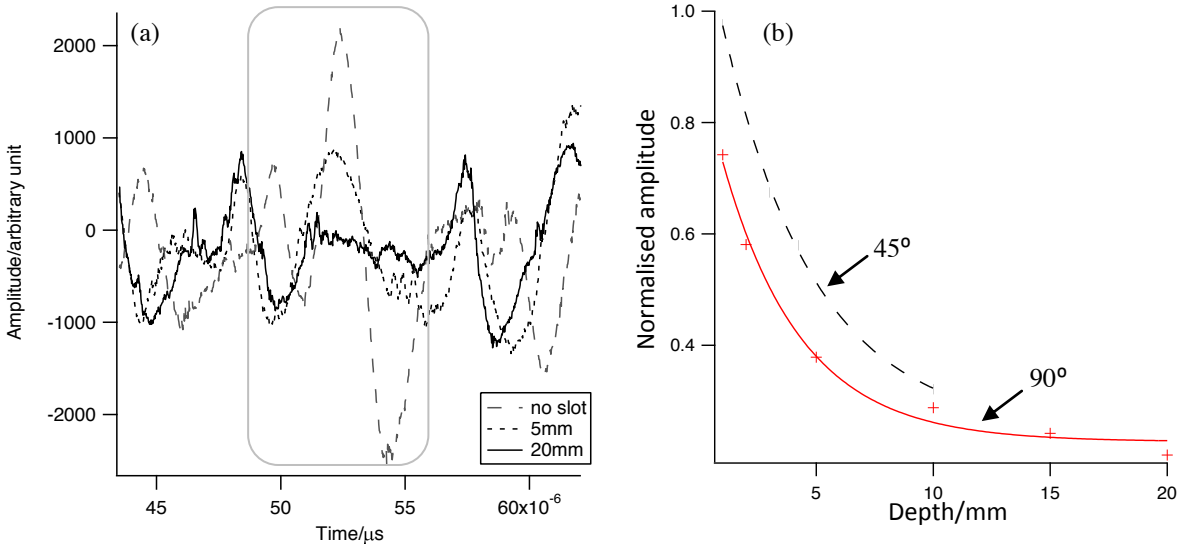

Figure 2 (a) Traces showing Rayleigh waves recorded from sample surface containing no slot, 5mm and 20mm normal slot (b) Depth calibration curve based on the amplitude measurement for normal (90°) and 45° slots.

Increasing separation of EMATs

The generation EMAT was fixed at 200mm from the slot opening and the detection EMAT was scanned from 150mm to 250mm away from the generation one with 0.5mm scan step. The scan was conducted using a stepper machine which controlled by a Labview program. At each position on the sample surface, the program records 20 signals and calculate the average. This helps to reduce noise from the stepper machine. Data recorded through the Labview program were analysed in IgorPro to generate B-scan. In B-scan, the grayscale represents the amplitude of the signal as shown in Figure 3. It runs from white (maximum positive) to black (maximum negative). Vertical axis shows the position of the detection EMAT relative to the slot opening while horizontal axis shows the arrival time. Rayleigh waves are shown by the brightest and darkest line indicated in region **B**. The B-scans show that there is a reflection of Rayleigh waves in region **C**. For normal slot, as the detection EMAT reaching the close proximity of the slot, these two waves start to interfere to each other and producing enhanced signals in region **A**. The position of the slot can be estimated to be about 3mm from where the interference occurs and when the reflections disappear i.e. between 0.197m and 0.200m.

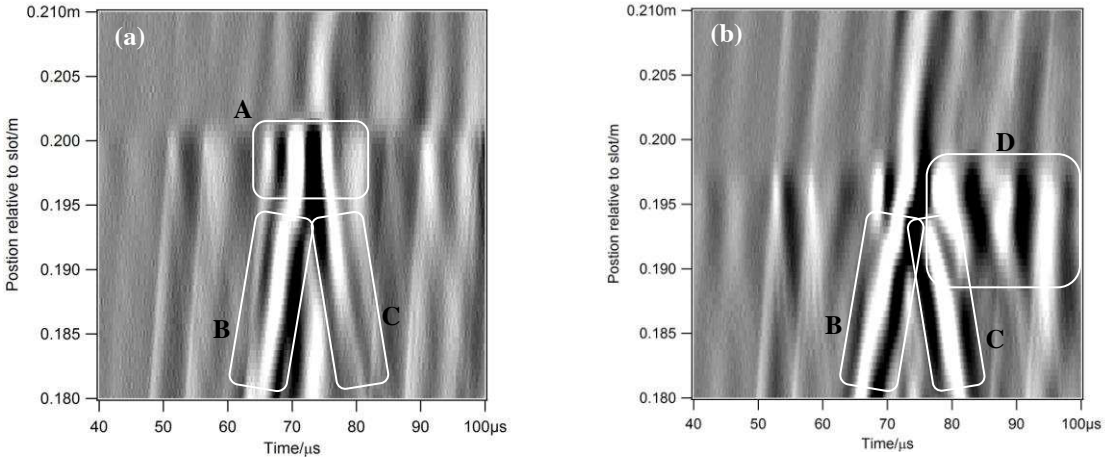

Figure 3 B-scans of two 5mm deep machine slots on aluminium bar (a) Normal (b) 22.5°.

On the other hand, the B-scans from angled slots show there are extra enhancement following the interference. For instance, Figure 3(b) shows the B-scan for a 5mm deep 22.5° slot. The mechanism behind the extra enhancement in region **D** is partly due to mode converted surface skimming longitudinal waves generated at the crack corner and partly due to interference of incident and reflected Rayleigh waves [13-15]. The differences in the enhancement pattern have been used as criteria to classify the type of the slots.

Fixed EMATs separation and scan using trolley

A pair of EMATs fixed on a trolley was scanned over various sample surfaces containing defects. In this case, the separation between the EMATs is fixed, hence incident Rayleigh waves arrive at the same time in the B-scans. As expected through the findings of preliminary experiment, the extra enhancement pattern have been observed when either EMAT is above an angled slot or crack. For instance, Figure 4(a) shows the B-scans of the test rail track containing three clusters of EDM notches. The presences of the clusters are indicated by six horizontal alternating black and white lines. The signals are enhanced whenever either EMAT pass over a cluster of notches. Thus, there are two lines for each cluster indicating when the generation or detection EMAT passing over.

Figure 4(b) shows the B-scan of a section of real rail tracks removed from service. As it shows, it is noisier than the scan made over aluminium samples. The amplitude of incident Rayleigh waves changes with the scan distance due to corrosion on the surface that varies the lift-off of EMATs. If the amplitude drops, it can be mistakenly understood as a small crack according to amplitude measurement. However, the results from the B-scan will indicate that is just a change in lift-off. Hence, unnecessary treatment of that section can be avoided.

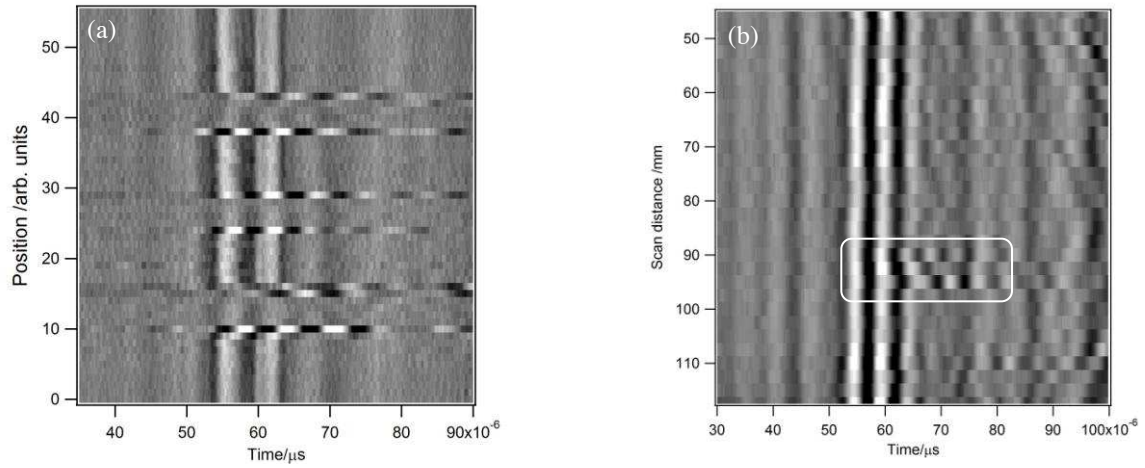

Figure 4 B-scans from (a) Test rail containing Electrical Discharge Machining notches and (b) Real rail defects.

IMAGE PROCESSING

The B-scan images are put into classes depending on presence/absence of defects and on defect type, either normal or angled. There are two major parts in the image processing package for the B-scans. First, a main program extracts features from a set of images and creates values associated with each image to form attributes. In the second part, the attributes are use for classification using an open source called Weka. The main program has been set up to read a set of B-scans from disk which is going to be classified. At the moment, there must an equal number of images from each class. There are 30 images in total, with 15 being normal cracks and 15 being angled cracks. The main program runs the images through a series of image processing steps, themselves are miniature programs. At the end of these, the miniature program outputs a numerical value. Therefore, for each miniature program, there are 30 values associated with 30 images. The quality of these is measured, and a new set of programs generated by mutation process. This is iterated many times in a process known as genetic programming. The representation of the program is in the form of mixture of functions that process images and mathematical functions, as illustrated in Figure 5.

The complete set of values for all the images is called a 'feature', consists of outputs from the various runs of the best version of the miniature programs. A number of these features are generated by the program, by running the genetic programming process multiple times and the collated into a spreadsheet in CSV format. Once the CSV file is generated, they are used as input for the classification algorithm using Weka [16]. Several classification algorithms can be ran against the CSV data file (neural network, decision tree induction algorithm). What Weka does with the CSV file is comparing the predicted classes according to the values of the various features to the actual class designated in the CSV file. In this way, we can tell whether the main program is creating features which can be used to accurately predict the class of images of this type [11]. So far, these image processing algorithms has 100% accuracy in classifying B-scan images from the experimental data. However, to get more realistic representation of surface defects, this program has to work on larger data set, especially from real crack or simulated machine slot on aluminium bars.

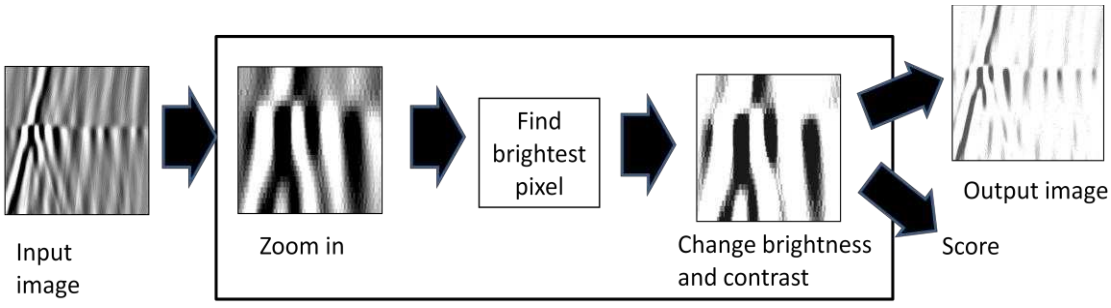

Figure 5 Example of image classification program creating values associated with the input image to form attributes.

CONCLUSION

Surface defects can be characterised through the analysis of Rayleigh waves amplitude and classification of B-scan images depending on their enhancement pattern. On small data set, the automated image classification program has 100% accuracy. In the future, we will increase the data set by doing more scans over various angled and normal cracks and defect-free surfaces on more realistic samples. The knowledge from this research can be implemented in identifying GCC on rails in order to reduce the risk of train derailment in the future.

REFERENCES

1. D. F. Cannon, K.-O. Edel , S. L. Grassie, K. Sawley, *Fatigue Fract Engng Mater Struct* **26**, 865-887 (2003).
2. R. A. Cottis, *Stress Corrosion Cracking*,Corrosion and Protection Centre, UMIST, Manchester, 2000.
3. G. Alers, "A History of EMATs", *Review of Quantitative Nondestructive Evaluation,* D. O. Thompson and D. E. Chimenti,AIP Conference Proceedings vol. 27, American Insitute of Physics, 2008, 801-808.
4. W.M. Irving, *Continuous Casting of Steel,* The Institute of Materials, London, 1993, 95-96
5. S. B. Palmer, S. Dixon, *Insight* **45**, 211-217 (2003).
6. M. Hirao, Hirotsugu Ogi, *EMATs for science and industry. Non-contact ultrasonic measurements,* Kluwer Academic Publisher, Boston/Dordrecht/London, 2003
7. R. S. Edwards, S.Dixon, X. Jian, *NDT&E International* **3**, 468-475 (2006).
8. T. Mitchell, *Machine Learning*, McGraw-Hill, 1997
9. K. Krawiec, "Visual Learning by Evolutionary Feature Synthesis", *Proceedings of the Twentieth International Conference on Machine Learning*, Tom Fawcett and Nina Mishra, AAAI Press, 2003, 376-383
10 S. Shirakawa, S. Nakayama, T. Nagao, "Genetic Image Network for Image Classification", *Application of Evolutionary Computing: EvoWorkshops 2009*, M. Giacobini, A. Brabazon, S. Cagnoni, et al., Springer Berlin/ Heidelberg 5484, 2009, 395-404
11. C. G. Johnson, P. Cattani, "Typed Cartesian Genetic Programming for Image Classification", *Proceeding of the 2009 UK Workshop on Computational Intelligence*, 2009
12. G. W. C. Kaye, T. H. Laby, *Tables of physical and chemical contstans 16th Ed*, Longman, (1995)
13. R.S. Edwards, X. Jian, Y. Fan, S. Dixon, *Applied Physics Letters* **87**, 194104 (2005).
14. X. Jian, S. Dixon, N. Guo, R. S. Edwards, M. Potter, *Ultrasonics* **44**, e1131-e1134 (2006)
15. R.S. Edwards, X. Jian, S. Dixon, *J. Phys. D: Appl. Phys.* **37,** 2291-2297 (2004).
16. I. H. Witten, E. Frank, *Data Mining*, Morgan Kaufmann, 2nd Edition, 2005